Journal of Enzyme Inhibition and Medicinal Chemistry, April 2005; 20(2): 135–141

Benzofuran- and furan-2-yl-(phenyl)-3-pyridylmethanols: Synthesis and inhibition of P450 aromatase

MOHAMMED R. SABERI†, KAJAL SHAH & CLAIRE SIMONS

Medicinal Chemistry Division, Welsh School of Pharmacy, Cardiff University, King Edward VII Avenue, Cardiff CF10 3XF, UK

(Received 15 June 2004; in final form 9 August 2004)

Abstract

A series of benzofuran-2-yl-(phenyl)-3-pyridylmethanol derivatives were prepared using an efficient 1-step procedure in good yields. In addition furan-2-yl-(phenyl)-3-pyridylmethanol derivatives were also prepared to determine the effect of the benzene ring in benzofuran with respect to inhibitory activity. The pyridylmethanol derivatives were all evaluated *in vitro* for inhibitory activity against aromatase ($P450_{AROM}$, CYP19), using human placental microsomes. The benzofuran-2-yl-(phenyl)-3-pyridylmethanol derivatives showed good to moderate activity ($IC_{50} = 1.3-25.1\,\mu M$), which was either better than or comparable with aminoglutethimide ($IC_{50} = 18.5\,\mu M$) but lower than arimidex ($IC_{50} = 0.6\,\mu M$), with the 4-methoxyphenyl substituted derivative displaying optimum activity. Molecular modelling of the benzofuran-2-yl-(4-fluorophenyl)-3-pyridylmethanol derivative suggested activity to reside with the (*S*)-enantiomer. The furan-2-yl-(phenyl)-3-pyridylmethanol derivatives were devoid of activity indicating the essential role of the benzene ring of the benzofuran component for enzyme binding.

Keywords: *Benzofuran-2-yl-(phenyl)-3-pyridylmethanols furan-2-yl-(phenyl)-3-pyridylmethanol derivatives, P450 aromatase, inhibitors, molecular modelling, proton affinity*

Introduction

The enzymes involved in the biosynthesis of steroidal hormones are proving to be major targets for therapeutic intervention[1]. One of these enzymes is aromatase ($P450_{Arom}$, CYP19), an enzyme complex consisting of a cytochrome P450 haemoprotein and an NADPH-cytochrome P450 reductase, which catalyses the final step in the steroidogenic pathway for the synthesis of oestrogens from cholesterol (Figure 1)[2].

A high proportion of breast tumours in post-menopausal women are dependent on oestrogen for growth and after surgery oestrogen deprivation strategies are used to prevent development of metastases. Aromatase inhibitors have been used in the clinic as second line drugs following relapse on tamoxifen therapy for this purpose[3].

Aromatase inhibitors have recently been highlighted as a result of publication of findings from clinical trials[4]. The so called "ATAC" (Arimidex, Tamoxifen, Alone or in Combination) trial suggested that aromatase inhibitors, specifically arimidex (**1**), may well be superior to tamoxifen (the current first-line therapy of choice) for the treatment of hormone-dependent breast cancer[5]. Studies have also indicated the use of aromatase inhibitors for preventive therapeutics, owing to their ability to reduce oestrogen levels; a high level of plasma oestrogen has been shown to be a high risk factor for subsequent breast cancer[6].

Correspondence: C. Simons, Medicinal Chemistry Division, Welsh School of Pharmacy, Cardiff University, King Edward VII Avenue, Cardiff CF10 3XF, UK. Tel: +44-(0)2920-876307. Fax: +44-(0)2920-874149. E-mail: SimonsC@Cardiff.ac.uk

†Present address: School of Pharmacy, Mashhad University of Medical Sciences, P.O. Box 91775-1365, Mashhad, I.R. Iran

ISSN 1475-6366 print/ISSN 1475-6374 online © 2005 Taylor & Francis Ltd
DOI: 10.1080/14756360400015256

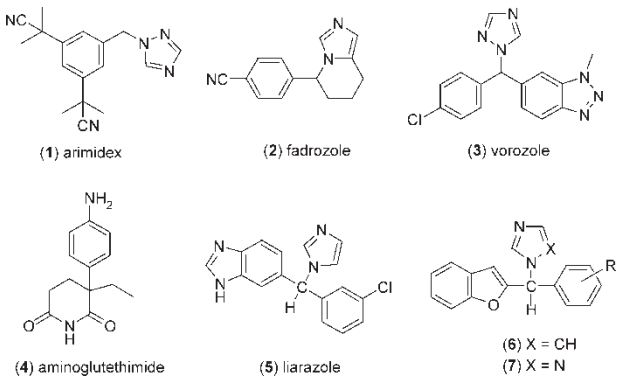

In addition to arimidex, several potent non-steroidal reversible inhibitors of the enzyme are known *e.g.* fadrazole (**2**) and vorozole (**3**), which are more specific inhibitors of the target enzyme[7] than the well established inhibitor aminoglutethimide (**4**, AG), and do not possess certain undesirable side effects of the latter[8]. Liarazole® (**5**), an azolyl-substituted benzimidazole[9], and the 1-[(benzofuran-2-yl)phenylmethyl]-imidazoles[10] (**6**) and triazoles[11] (**7**), are also potent $P450_{AROM}$ inhibitors. These inhibitors bind to the active site of $P450_{AROM}$ through coordination of a heterocyclic nitrogen lone pair of electrons with the Fe^{3+} of the haem in the active site of the enzyme, therefore the coordination potential of the heterocyclic nitrogen is of importance. We have previously shown that, with respect to coordination potential/inhibitory activity, an imidazole is more efficient than a triazole, which is more efficient than a tetrazole heterocyclic moiety[12]. However, imidazole derivatives may also be less selective compared with triazole derivatives, which are also more stable metabolically. It was of interest to study the effect of introducing a pyridine heterocyclic moiety into the benzofuran series (**8**) on inhibitory activity. Owing to the availability of the lone pair of the pyridine nitrogen and calculated proton affinities it was expected that activity would fall between that of the triazole and tetrazole derivatives.

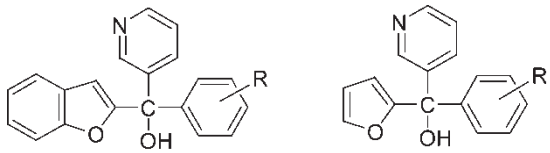

In addition two furan derivatives (**9**) were also prepared to assess the role of the benzene component of the benzofuran ring in enzyme binding.

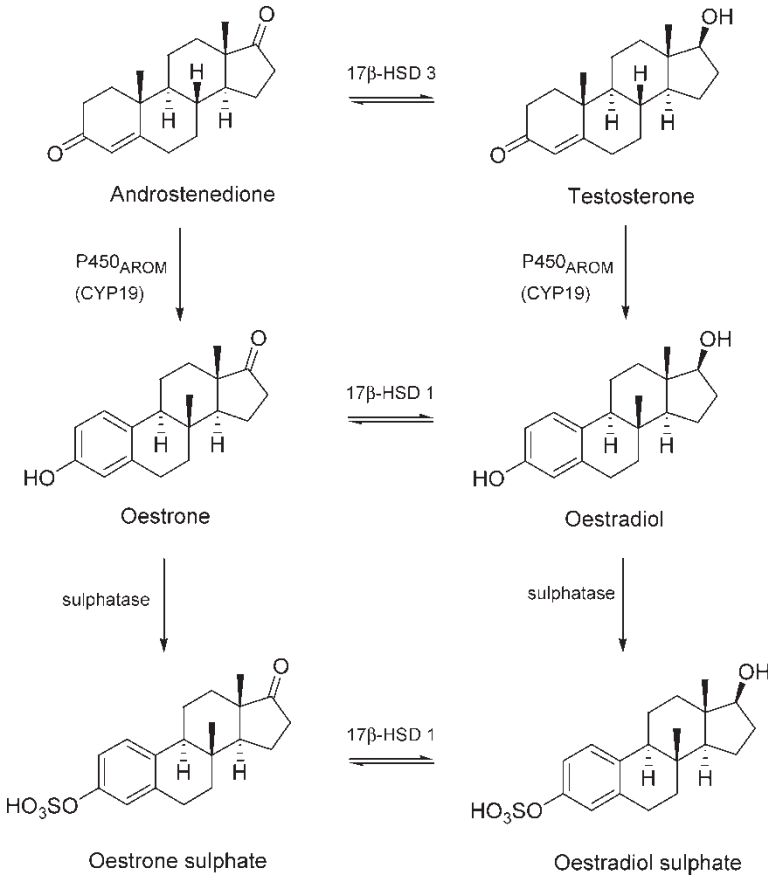

Figure 1. Steroidogenesis pathway for the generation of oestrogens.

Materials

^{1}H and ^{13}C NMR spectra were recorded with a Brucker Avance DPX300 spectrometer operating at 300 and 75 MHz respectively, in DMSO-d_6 with Me_4Si as internal standard. Chemical shifts are expressed in parts per million downfield from TMS. Microanalyses were determined by Medac Ltd., Surrey. Mass spectroscopy was performed at the EPSRC Mass Spectroscopy Centre, Swansea University. Flash column chromatography was performed with silica gel 60 (230–400 mesh) (Merck) and TLC was carried out on precoated silica plates (kiesel gel 60 F_{254}, BDH). Melting points were measured with a Gallenkamp Melting Point Apparatus and are reported uncorrected. All the reactions were carried out under nitrogen using anhydrous solvents. Gaussian98W software was obtained from Gaussian, Inc. Pittsburgh USA.

[1,2,6,7-^{3}H]androstenedione (86.4 Ci/mmol–37 MBq/mL) was purchased from NEN-Dupont UK (Stevenage, Herts). Scintillation fluid was Optiphase Hisafe from Fisons Chemicals (Loughborough, UK). The scintillation counter used was a LKB Wallac, 1217, Rack-beta.

Methods

Chemistry

Compounds **10a**–**10f** and **11a** and **11b** were prepared according to reported methods[11,13–15]. Compounds **8a**–**8f**, **9a** and **9b** were prepared according to the following procedures.

General method for the preparation of benzofuran-2-yl-(phenyl)-3-pyridylmethanols 8a–8f and furan-2-yl-(phenyl)-3-pyridylmethanols 9a and 9b. To a solution of pyridin-3-magnesium bromide (20 mmol) in THF (30 mL), generated *in situ* by the reaction of pyridin-3-bromide (20 mmol), dry magnesium turnings (20 mmol) in THF (30 mL) under reflux for 1 h, was added the ketone **10** or **11** (5 mmol) and the reaction heated at 70 °C for 1 h. The solvent was removed under reduced pressure and the resulting residue dissolved in CH_2Cl_2 (50 mL), washed with H_2O (30 mL), dried ($MgSO_4$) and concentrated under reduced pressure. The crude product was purified by flash column chromatography (petroleum ether–ethyl acetate 8:2 increasing to 7:3 v/v) followed by recrystallisation to give the target compound.

*Benzofuran-2-yl-(4-Fluoro-Phenyl)-3-Pyridylmethanol **8a**.* White crystalline solid (75%), mp 50–54 °C (petroleum ether). ^{1}H NMR δ 8.48 (apparent t, J = 1.6 Hz, 1H, Ar), 8.43 (dd, J = 1.5, 4.8 Hz, 1H, Ar), 7.68 (dt, J = 3.9, 8.0 Hz, 1H, Ar), 7.47 (m, 1H, Ar), 7.35 (m, 1H, Ar), 7.25 (m, 5H, Ar), 6.68 (m, 2H, Ar), 6.28 (d, J = 0.7 Hz, 1H, CH furan), 4.61 (s, 1H, OH); ^{13}C NMR δ 161.2 (C), 159.5 (C), 155.6 (C), 149.2 (CH), 149.0 (CH), 140.2 (C), 139.65 (C), 135.5 (CH), 129.6 (CH), 129.5 (CH), 128.0 (C), 125.3 (CH), 123.6 (CH), 123.5 (CH), 121.9 (CH), 115.8 (CH), 115.5 (CH), 111.8 (CH), 107.1 (CH), 76.9 (C—OH). MS (EI) *m/z*: 319.0 (M^+). Found: C, 75.12; H, 4.20; N, 4.20. $C_{20}H_{14}NO_2F$ (319.34) requires: C, 75.23; H, 4.42; N, 4.38%.

*Benzofuran-2-yl-(4-Chloro-Phenyl)-3-Pyridylmethanol **8b**.* White crystalline solid (70%), mp 102–104 °C (petroleum ether). ^{1}H NMR δ 8.56 (d, J = 2.1 Hz, 1H, Ar), 8.52 (dd, J = 1.4, 4.8 Hz, 1H, Ar), 7.78 (dt, J = 1.9, 8.0 Hz, 1H, Ar), 7.57 (dd, J = 1.8, 7.0 Hz, 1H, Ar), 7.45 (d, J = 8.0 Hz, 1H, Ar), 7.34 (m, 7H, Ar), 6.40 (d, J = 0.4 Hz, 1H, CH furan), 4.86 (s, 1H, OH); ^{13}C NMR δ 159.3 (C), 155.6 (C), 149.2 (CH), 148.9 (CH), 142.4 (C), 140.1 (C), 135.6 (CH), 134.6 (C), 129.1 (CH), 128.9 (CH), 128.0 (C), 125.4 (CH), 123.7 (CH), 123.5 (CH), 121.9 (CH), 111.9 (CH), 107.2 (CH), 76.9 (C—OH). Found: C, 71.47; H, 4.18; N, 4.05. $C_{20}H_{14}NO_2Cl$ (335.78) requires: C, 71.54; H, 4.20; N, 4.17%.

*Benzofuran-2-yl-(4-Bromo-Phenyl)-3-Pyridylmethanol **8c**.* White crystalline solid (70%), mp 72–74 °C (petroleum ether). ^{1}H NMR δ 8.51 (d, J = 1.4, 2H, Ar), 7.81 (dd, J = 1.6, 8.0 Hz, 1H, Ar), 7.54 (d, J = 6.8 Hz, 1H, Ar), 7.41 (d, J = 7.0 Hz, 1H, Ar), 7.27 (m, 5H, Ar), 6.89 (d, J = 5.5 Hz, 2H, Ar), 6.39 (s, 1H, CH furan), 5.35 (s, 1H, OH). ^{13}C NMR δ 159.7 (C), 155.6 (C), 149.0 (CH), 148.7 (CH), 140.8 (C), 136.3 (C), 135.7 (CH), 129.0 (CH), 129.0 (C), 128.2 (C), 125.0 (CH), 123.5 (CH), 123.4 (CH), 121.8 (CH), 114.0 (CH), 111.9 (CH), 106.8 (CH), 55.7 (C—OH). MS (EI) *m/z*: 380.0 $(M + H)^+$. Found: C, 63.15; H, 3.68; N, 3.65. $C_{20}H_{14}NO_2Br$ (379.02) requires: C, 63.18; H, 3.71; N, 3.68%.

*Benzofuran-2-yl-(4-Iodo-Phenyl)-3-Pyridylmethanol **8d**.* Off-white crystalline solid (75%), mp 119–122 °C (petroleum ether). ^{1}H NMR δ 8.45 (d, J = 2.3 Hz, 1H, Ar), 8.38 (dd, J = 1.5, 4.8 Hz, 1H, Ar), 7.75 (dt, J = 6.5 Hz, 1H, Ar), 7.68 (d, J = 8.5 Hz, 2H, Ar), 7.55 (m, 1H, Ar), 7.30 (m, 4H, Ar), 7.14 (d, J = 8.6 Hz, 2H, Ar), 6.39 (s, 1H, CH furan), 6.70 (s, 1H, OH). ^{13}C NMR δ 159.47 (C), 155.63 (C), 148.72 (CH), 148.61 (CH), 143.84 (C), 140.44 (C), 137.79 (CH), 135.78 (CH), 129.64 (CH), 128.00 (C), 125.26 (CH), 123.63 (CH), 123.54 (CH), 121.86 (CH), 111.88 (CH), 107.12 (CH), 94.56 (C), 53.92 (C—OH). Found: C, 56.03; H, 3.26; N, 2.91. $C_{20}H_{14}NO_2I$ (427.24) requires: C, 56.23; H, 3.30; N, 3.28%.

*Benzofuran-2-yl-(2,4-Dichloro-Phenyl)-3-Pyridylmethanol **8e**.* Yellow crystalline solid (58%), mp 82–84 °C (petroleum ether). ^{1}H NMR δ 8.58 (d, J = 1.7 Hz, 1H, Ar), 8.48 (dd, J = 1.6, 4.8 Hz, 1H, Ar), 7.85

(dt, $J = 1.9$, 8.0 Hz, 1H, Ar), 7.57 (dd, $J = 2.1$, 6.8 Hz, 1H, Ar), 7.4 (m, 8H, Ar), 6.45 (d, $J = 0.7$, 1H, CH furan), 6.10 (s, 1H, OH). ^{13}C NMR δ 158.33 (C), 155.53 (C), 148.81 (CH), 148.65 (CH), 139.66 (C), 139.18 (C), 135.56 (CH), 135.49 (C), 134.48 (C), 131.84 (CH), 131.41 (CH), 129.50 (CH), 128.69 (C), 128.10 (C), 127.37 (C), 125.27 (CH), 123.68 (CH), 123.49 (CH), 121.95 (CH), 112.00 (CH), 107.26 (CH), 76.30 (C—OH). Found: C, 64.89; H, 3.68; N, 3.77. $C_{20}H_{13}NO_2Cl_2$ (370.23) requires: C, 64.88; H, 3.54; N, 3.78%.

Benzofuran-2-yl-(4-Methoxy-Phenyl)-3-Pyridyl-methanol ***8f***. White crystalline solid (50%), mp 102–104°C (petroleum ether). ^{1}H NMR δ 8.45 (dd, $J = 1.5$, 5.9 Hz, 1H, Ar), 7.82 (d, $J = 1.4$, Hz, 1H, Ar), 7.54 (d, $J = 8.0$ Hz, 1H, Ar), 7.35 (m, 5H, Ar), 7.10 (m, 4H, Ar), 6.40 (d, $J = 0.5$ Hz, 1H, CH furan), 4.80 (s, 1H, OH), 4.21 (s, 3H, CH_3). ^{13}C NMR δ 159.5 (C), 153.7 (C), 152.2 (CH), 146.8 (CH), 140.4 (C), 140.1 (C), 137.7 (CH), 134.1 (C), 131.1 (CH), 127.3 (CH), 128.2 (C), 127.9 (CH), 122.5 (CH), 122.1 (CH), 121.1 (CH), 113.9 (CH), 106.8 (CH), 76.7 (C—OH), 55.7 (CH_3). Found: C, 76.01; H, 4.98; N, 4.45. $C_{21}H_{17}NO_3$ (331.36) requires: C, 76.12; H, 5.17; N, 4.23%.

Furan-2-yl-(4-Chloro-Phenyl)-3-Pyridylmethanol ***9a***. White crystalline solid (78%), mp 42–43 °C (petroleum ether). ^{1}H NMR δ 8.38 (dd, $J = 2.4$, 2.8 Hz, 1H, Ar), 8.36 (d, $J = 1.5$ Hz, 1H, Ar), 7.72 (dt, $J = 1.8$, 8.0 Hz, 1H, Ar), 7.42 (ψt, $J = 0.6$, 1.0 Hz, 1H, Ar), 7.28 (m, 5H, Ar), 6.36 (dd, $J = 1.8$, 3.3 Hz, 1H,Ar), 5.98 (dd, $J = 0.6$, 3.3 Hz, 1H, Ar), 5.55 (s, 1H, OH). ^{13}C NMR δ 157.5 (C), 148.3 (CH), 147.9 (CH), 143.7 (CH), 143.3 (C), 141.5 (C), 135.81 (CH), 134.0 (C), 129.1 (CH), 128.6 (CH), 123.5 (CH), 110.6 (CH), 110.1 (CH), 76.1 (C—OH). Found: C, 66.56; H, 4.19; N, 4.86. $C_{16}H_{12}ClNO_2 \cdot 0.1\ H_2O$ (287.530) requires: C, 66.84; H, 4.28; N, 4.87%.

Furan-2-yl-(4-Methoxy-Phenyl)-3-Pyridylmethanol ***9b***. Colourless syrup (50%). ^{1}H NMR δ 8.45 (d, $J =$ 1.9 Hz, 1H, Ar), 8.35 (dd, $J = 1.3$, 4.8 Hz, 1H, Ar), 7.75 (dt, $J = 1.9$ Hz, 1H, Ar), 7.40 (m, 1H, Ar), 7.22 (m, 3H, Ar), 6.87 (ψt, $J = 2.0$, 2.9 Hz, 1H, Ar), 6.84 (ψt, $J = 1.9$, 3.0 Hz, 1H, Ar), 6.33 (dd, $J = 1.8$, 3.2 Hz, 1H, Ar), 5.96 (d, $J = 3.2$ Hz, 1H, Ar), 5.29 (s, 1H, OH), 3.81 (s, 3H, CH_3). ^{13}C NMR δ 159.5 (C), 158.0 (C), 148.8(CH), 148.3 (CH), 143.2 (C), 141.5 (CH), 137.0 (C), 135.6 (CH), 128.9 (CH), 123.3 (CH), 113.8 (CH), 110.5 (CH), 109.9 (CH), 76.5 (C—OH), 55.7 (CH_3). MS (ES +) *m/z*: 281.0 (M^+).

Preparation of human placental microsomes

Freshly delivered full-term placenta was removed of connective tissue and then cut into small pieces and stored in ice. The placenta was washed with Tris pH 7.4 buffer, containing 25 mM KCl, 5 mM MgCl and 0.25 mM sucrose, and initially blended to a fine consistency using a commercial food blender. The blended placenta was then homogenised using a Potter-Elvejhem homogeniser. The homogenate was centrifuged at 12,000 rpm for 15 min at 4 °C using a Sorvall OTD ultracentrifuge, then the supernatant ultracentrifuged at 38,000 rpm for 60 min at 4 °C. The resulting pellets, the microsomal fraction, were dispersed in Tris buffer using a homogeniser then stored in vials at −80 °C. Protein concentration of the microsomal fraction was determined using the Pierce BCA protein assay.

Aromatase assay

The classical ^3H_2O assay[16] was used to measure the effect of the inhibitor compounds on aromatase activity using human placental microsomes. A solution of [1,2,6,7-^{3}H]androstenedione and androstenedione (0.5 μM final concentration) was incubated in test tubes at 37 °C for 15 min with the human placental microsomal preparation (8.24 mg/mL, 30 μL), phosphate buffer (400 μL, 50 mM, pH 7.4) and NADPH (50 μL, 16 mM) in the presence of inhibitor (10 μL, 1 or 5 mmol–20 or 100 μM final concentration respectively) in EtOH. Control experiments were run with EtOH (10 μL) in place of the inhibitor. The reaction was quenched by the addition of aqueous $HgCl_2$ (30 μL, 1 mM) followed by an aqueous suspension of charcoal (1 mL, 1% by weight). The test tubes were centrifuged (15 min, 3000 rpm), then the supernatant liquid placed in a scintillation vial to which 1 mL of scintillation fluid was added. The ^3H_2O contained in each vial was then determined using a LKB Wallac, 1217, Rack-beta scintillation counter.

For IC_{50} values the general method described for determination of percentage inhibition was followed except that a range of concentrations of inhibitor were used. Calculation of IC_{50} was determined by plotting % inhibition *versus* Log [I] using Cricket Graph III 1.5f software[17].

Ab initio

All *ab initio* calculations were performed using Gaussian98W[18] running on a P3 PC. The geometries of the benzofuran derivatives were optimised at the HF/6-31G(d) level to obtain global minima with subsequent single point calculations for energies and properties[19].

Results and discussion

Chemistry

Preparation of the benzofuran-2-yl-(phenyl)-3-pyridylmethanols **8a**–**8f** was achieved by reaction of the

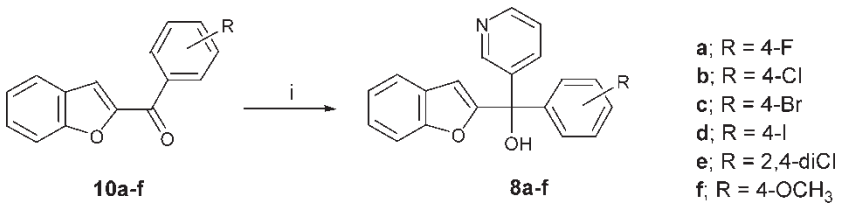

Scheme 1. Reagents and conditions: (i) Pyridine-3-bromide, Mg, THF, crystal I_2, 70 °C, 1 h then 10, 70 °C, 1 h.

corresponding ketones[11,13] **10** with the Grignard reagent pyridin-3-magnesium bromide, which was generated *in situ* from commercially available pyridin-3-bromide and magnesium in the usual manner (Scheme 1). The racemic pyridylmethanols were obtained in moderate to good yields (Table I), after purification by column chromatography and subsequent recrystallisation.

Likewise the racemic furan-2-yl-(phenyl)-3;-pyridylmethanols **9a** and **9b** were obtained by reaction of the furan-2-yl-(phenyl)methanones[14,15] **11a** and **11b** respectively with the Grignard reagent, pyridin-3-magnesium bromide (Scheme 2).

Inhibitory activity

The pyridylmethanols **8** and **9** were all evaluated *in vitro* for inhibitory activity against aromatase ($P450_{AROM}$, CYP19), using human placental microsomes. From this small library of compounds, some preliminary SAR data can be deduced. The presence of the phenyl ring has previously been shown to be important for inhibitory activity in the 1-[(benzofuran-2-yl)phenyl]imidazole series[20], a similar importance was noted for the benzene ring of the benzofuran structure. Removal of the benzene ring of the benzofuran component (furans **9a** and **9b**) resulted in a loss of activity (Table I), indicating the requirement of an aromatic group at this position for hydrophobic/$\pi - \pi$ interactions with the active site. In the benzofuran pyridyl series (Figure 2) a large atom in the 4-position of the phenyl ring was detrimental to activity, with the 4-bromo-phenyl (**8c**, $IC_{50} = 25.1\,\mu M$) and 4-iodo-phenyl (**8d**, $IC_{50} = 12.8\,\mu M$) derivatives displaying activity comparable with aminoglutethimide.

Table I. Yields, mp values and IC_{50} data for **8a**–**8f**, **9a**–**9b**.

Compound	R	Yield (%)	mp (°C)	IC_{50} (μM)[a]
8a	4-F	75	50–54	7.0
8b	4-Cl	70	102–104	4.3
8c	4-Br	70	72–4	25.1
8d	4-I	75	119–122	12.8
8e	2,4-diCl	58	82–84	2.2
8f	4-OCH_3	50	102–104	1.3
9a	4-Cl	78	42–43	> 100
9b	4-OCH_3	50	–	> 100
AG	–	–	–	18.5
Arimidex	–	–	–	0.6

Concentration of androstenedione, 0.5 μM. IC_{50} values are the average (±5%) of two experiments.

Substitution of the phenyl ring with the smaller halogens, 4-fluoro-phenyl (**8a**, $IC_{50} = 7.0\,\mu M$) and 4-chloro-phenyl (**8b**, $IC_{50} = 4.3\,\mu M$) resulted in increased activity. These findings, F/Cl > Br/I with respect to $P450_{AROM}$ inhibitory activity, were consistent with the model of Laughton et al[21], which indicated steric restrictions in the left-hand pocket of the aromatase active site.

The increased activity observed with the 2,4-dichloro-phenyl derivative (**8e**, $IC_{50} = 2.2\,\mu M$) may be owing to the molecule being held in a more favourable position for binding, owing to steric hinderance between the 2-chloro substituent on the phenyl ring and the pyridyl ring. The optimum activity was observed for the 4-methoxy-phenyl derivative (**8f**, $IC_{50} = 1.3\,\mu M$), this may well be owing to the methoxy group interacting with a hydrogen bonding group, as described by Laughton *et al*, within this area of the active site.

Computational analysis

Using an aromatase model, built with Swiss-PdB software[22] using P450cam (1cpt PDB code[23]) as the template, the geometry optimised structures of the (*R*)- and (*S*)-enantiomeric forms of the 4-fluorophenyl derivative, benzofuran-2-yl-(4-fluoro-phenyl)-3-pyridinylmethanol (**8a**) were docked into the active site with the nitrogen of pyridine positioned toward the iron atom of the haem and the benzofuran and phenyl ring optimally positioned in the cavity. Energy minimisation using the Amber94 forcefield (SwissPdbViewer program) provided the most suitable final conformation of the enzyme and ligand (Figure 3).

The (*R*)-enantiomer that directs the phenyl ring to the back (*i.e.* near amino acid residue Glu302) suffered from serious steric clashes of both the benzofuran and phenyl rings with the proximal amino acids. In contrast, the (*S*)-enantiomer solved both problems and put the phenyl ring in a cavity made by Leu119, Leu474, Asp371 and Val373 where the closest residue was Val373 (4.64 Å proximity). The nitrogen atom of pyridine was 3.25 Å from the iron atom on the haem, *i.e.* capable of forming a coordinate bond. The benzofuran ring may interact

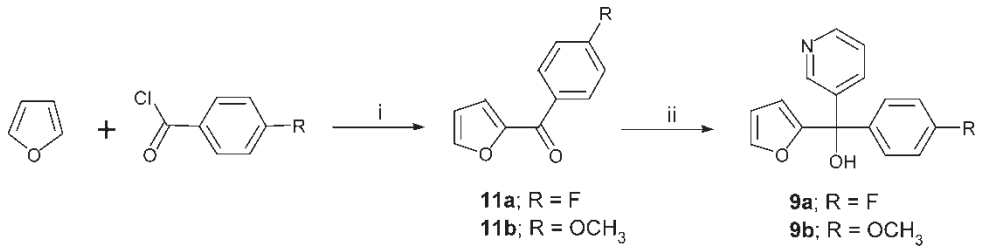

Scheme 2. Reagents and conditions: (i) CS_2, $AlCl_3$, room temperature o/n then 34 °C, 4 h (ii) pyridine-3-bromide, Mg, THF, crystal I_2, 70 °C, 1 h then 11, 70 °C, 1 h.

with the active site via the oxygen atom of the benzofuran system (Asp309) however more important contributions are expected to arise from hydrophobic interactions with appropriate aromatic amino acid side chains. No obvious interactions for the C1—OH group were observed with this model. This result was in contrast to an earlier computational study with 1-[(benzofuran-2-yl)phenylmethyl]imidazole[24], which found that both the (*R*)- and (*S*)-enantiomers gave a good fitting pattern, possibly indicating that the additional size of the pyridyl ring may orientate the molecule in a less favourable binding conformation for the (*R*)-enantiomer.

Proton affinity was used as a measure of binding capability to rationalise the interaction of the nitrogen heteroatom of the various nitrogen-containing heterocycles with the Fe^{3+} atom of the active site haem. Proton affinity (PA) was computed as the energy difference between the benzofuran derivative (R) and the same molecule with one additional proton (RH +) on the coordinating nitrogen, *i.e.* PA = E(R) − E(RH+) (Table II). *Ab initio* calculations were performed using Gaussian98W, the geometries of the compounds were optimised at the RHF/6-31d level with single point calculations to obtain more accurate energies and properties. In all cases the (*S*)-enantiomer was used with the 4-fluorophenyl substitution.

From computational models, activity would be predicted to reside in the (*S*)-enantiomer of the pyridylmethanol benzofuran derivatives (**8a**–**8f**), with optimal activity observed for the 4-methoxy derivative. The activity of the benzofuran derivatives has been shown to be dependent on the basicity of the nitrogen heterocycle with inhibitory activity decreasing with decreasing basicity (pKa: imidazole, 14.5 > triazole, 10 > pyridine, 5.2 > tetrazole, 4.8), which correlates well with the proton affinities (imidazole, PA = 247 $kJmol^{-1}$ > triazole, PA = 231 $kJmol^{-1}$ > pyridine, PA = 206 $kJmol^{-1}$ > tetrazole, PA = 226 $kJmol^{-1}$), with the exception of the pyridyl moiety which would be predicted from proton affinity to have lower binding affinity for the haem, for these heterocyclic moieties as determined by *ab initio* calculations of total E (ΔE) (Table II). The *ab initio* data does not account for the basicity and increased

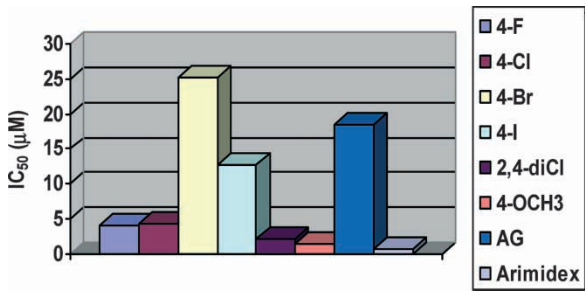

Figure 2. IC_{50} data for pyridyl benzofurans **8a**–**8f**.

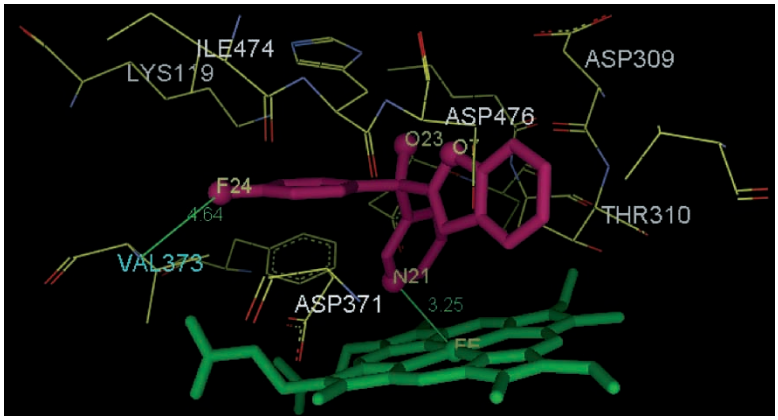

Figure 3. (*S*)-Enantiomer of benzofuran-2-yl-(4-fluoro-phenyl)-3-pyridinylmethanol (pink) in the active site. The more important residues have been labelled. The nitrogen atom of pyridine lies 3.25 Å from the ferric atom of the haem (green).

Table II. Proton affinity and dipole moment determined by *ab intio* calculations

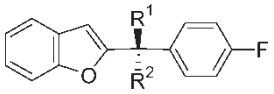

Molecule	E(RHF)/hartree*	PA(kcal mol^{-1})	Dipole (D) X, Y, Z, Total
Imidazole (R^1 = imidazole, R^2 = H)	−972.3763	247.11	2.2557, −1.6109, 1.9057, 3.3637
ImidazoleH + (R^1 = imidazoleH$^+$, R^2 = H)	−972.7701		−2.7819, 10.0268, −0.1133, 10.4062
Triazole (R^1 = triazole, R^2 = H)	−988.3691	230.61	1.7345, −0.7128, 1.3612, 2.3172
TriazoleH + (R^1 = triazoleH$^+$, R^2 = H)	−988.7366		−3.7013, 13.9972, 2.2286, 14.6488
Pyridine (R^1 = pyridyl, R^2 = OH)	−1069.1070	205.64	1.5933, 0.6898, 0.5871, 1.8328
PyridineH + (R^1 = pyridylH$^+$, R^2 = OH)	−1069.4947		−4.5601, 13.0696, −0.7018, 13.8601
Tetrazole (R^1 = tetrazole, R^2 = H)	−1004.3188	226.41	2.5264, −2.7849, 3.4490, 5.1023
TetrazoleH + (R^1 = tetrazoleH$^+$, R^2 = H)	−1004.6796		1.1691, 9.5017, 3.3209, 10.1330

*E(RHF) = total energy for Restricted Hartree-Fock calculation, 1 hartree = 627.51 kcal mol^{-1}.

size of the pyridyl moiety which might result in a closer interaction with the haem Fe^{3+}. On protonation the dipole moment is, as expected, mainly along the Y-axis, pointing towards the positively charged protonated nitrogen, with negative contributions along the X-axis (from the benzofuran oxygen) for the imidazole, triazole and pyridyl derivatives (−2.8, −3.7 and −4.6 debye respectively) (Table II).

Acknowledgements

One of us (MRS) would like to thank Mashhad University of Medical Sciences (MUMS) and the Iranian Ministry of Health for the award of a PhD scholarship. We would also like to acknowledge the EPSRC Mass Spectrometry Centre, Swansea, UK for mass spectroscopy data, the Royal Society for the award of an equipment grant for the purchase of computer hardware and software (ChemDraw Ultra 7.0 and Gaussian98W), and Astra Zeneca for the kind gift of Arimidex.

References

[1] Smith HJ, Nicholls PJ, Simons C, Le Lain R. Exp Opin Ther Pat 2001;11:789–824.
[2] Banting L In: Ellis GP, Luscombe DK, editors. In Progress in Medicinal Chemistry. Amsterdam: Elsevier Science; 1996. Vol. 33, p 147–184.
[3] Brodie A In: Sandler M, Smith HJ, editors. In Design of Enzyme Inhibitors as Drugs. Oxford: Oxford University Press; 1994. Vol. 2, p 424–438.
[4] Lønning PE. BMJ 2001;323:880–881.
[5] Goss PE, Strasser K. J Clin Oncol 2001;19:881–894.
[6] Key TJ. Endocr Relat Cancer 1999;6:175–180.
[7] Miller WR. Endocr Relat Cancers 1996;3:65–79.
[8] Shaw MA, Nicholls PJ, Smith HJ. J Steroid Biochem 1988;31:137–146.
[9] De Coster R, Wouters W, Bowden CR, Bossche HV, Bruynseels J, Tuman RW, Vanginkel R, Snoek E, Vanpeer A, Janssen PAJ. J Steroid Biochem Molec Biol 1990;37:335–341.
[10] Whomsley R, Fernandez E, Nicholls PJ, Smith HJ, Lombardi P, Pestellini V. J Steroid Biochem Molec Biol 1993;44:675–676.
[11] Vinh TK, Yee SW, Kirby AJ, Nicholls PJ, Simons C. Anticancer Drug Design 2001;16:217–225.
[12] Vinh TK, Ahmadi M, Lopez Delgado PO, Fernandez Perez S, Walters HM, Smith HJ, Nicholls PJ, Simons C. Bioorg Med Chem Lett 1999;9:2105–2108.
[13] Bisagni AF, J Chem Soc 1955;:3603.
[14] Fayed S, Delmas M, Gaset A. Synth Commun 1982;12:1121–1126.
[15] Gilman H, Rowe LW, Dickey JB. Rec Trav Chim Pays-Bas 1933;52:395–398.
[16] Thompson WA, Siiteri PK. J Biol Chem 1974;249:5364–5372.
[17] http://www.epinions.com/Computer_Associates_International__Inc__CA-Cricket_Graph_III_S0099584
[18] http://www.gaussian.com/
[19] Foresman JB, Frisch A. Exploring Chemistry With Electronic Structure Methods. 2nd ed. Pittsburgh USA: Inc. Gaussian, 1996.
[20] Khodarahmi GA, Smith HJ, Nicholls PJ, Ahmadi M. J Pharm Pharmacol 1998;50(Supplement),207.
[21] Laughton CA, Zvelebil MJ, Neidle S. J Steroid Biochem Mol Biol 1993;44:399–407.
[22] Guex N, Peirsch M, Torsten S. Diemand A. (2001) Swiss-Pdb Viewer. 3.7th ed. GlaxoSmithKline. http:/ca.expasy.org/spdbv/
[23] Hasemann CA, Ravichandran KG, Peterson JA. Deisenhofer J, J Mol Biol 1994;236:1169–1185.
[24] Khodarahmi GA, Laughton CA, Smith HJ, Nicholls PJ. J Enz Inhib 2001;16:401–416.